TOPICAL REVIEW

Through the eye of the needle: recent advances in understanding biopolymer translocation

IOP PUBLISHING JOURNAL OF PHYSICS: CONDENSED MATTER

J. Phys.: Condens. Matter **25** (2013) 413101 (15pp) doi:10.1088/0953-8984/25/41/413101

TOPICAL REVIEW

Through the eye of the needle: recent advances in understanding biopolymer translocation

Debabrata Panja[1,2], **Gerard T Barkema**[1,3] **and Anatoly B Kolomeisky**[4]

[1] Institute for Theoretical Physics, Universiteit Utrecht, Leuvenlaan 4, 3584 CE Utrecht, The Netherlands
[2] Institute for Theoretical Physics, Universiteit van Amsterdam, Science Park 904, Postbus 94485, 1090 GL Amsterdam, The Netherlands
[3] Instituut-Lorentz, Universiteit Leiden, Niels Bohrweg 2, 2333 CA Leiden, The Netherlands
[4] Department of Chemistry, Rice University, 6100 Main Street, Houston, TX 77005-1892, USA

E-mail: D.Panja@uu.nl

Received 10 May 2013
Published 11 September 2013
Online at stacks.iop.org/JPhysCM/25/413101

Abstract
In recent years polymer translocation, i.e., transport of polymeric molecules through nanometer-sized pores and channels embedded in membranes, has witnessed strong advances. It is now possible to observe single-molecule polymer dynamics during the motion through channels with unprecedented spatial and temporal resolution. These striking experimental studies have stimulated many theoretical developments. In this short theory–experiment review, we discuss recent progress in this field with a strong focus on non-equilibrium aspects of polymer dynamics during the translocation process.

(Some figures may appear in colour only in the online journal)

Contents

1. Introduction

Translocation, commonly understood to be the transport of polymeric molecules through nanometer-sized pores and channels (nanopores and nanochannels in short) embedded in membranes, and related dynamic phenomena in confined geometries are of fundamental and critical importance for many processes in chemistry, physics and biology, as well as for many industrial and technological applications [1–6]. In

the last two decades significant progress has been achieved in experimental studies of the translocation process at the single-molecule level [2, 4, 6–13]. This has opened up the opportunity for the development of nanopore devices as a new class of chemical and biological sensors. Experimental successes have naturally stimulated significant theoretical efforts to understand mechanisms of polymer dynamics in nanopores and nanochannels [2, 3, 14–17], although many questions remain unanswered.

In vivo, translocation of biological molecules is assisted by interactions with cellular membranes and/or special protein molecules [1]. *In vitro*, (bio)polymers are driven across pores or channels by applying external fields in single-molecule experiments [2–4, 6–11]. The pores or channels connect two compartments that are separated by an otherwise impenetrable membrane. A voltage difference is applied between the two compartments, which would normally cause the flow of an ionic current through the pore. When a polymer enters the pore, it partly blocks the path of the ions, resulting in a 'current blockade', a significant decrease in the ionic current. The polymer makes many attempts to cross the pore; the unsuccessful attempts result in current blockades of very short durations, which are digitally filtered out. In the experiments the actual translocation events are associated with the longer blocked current signals (figure 1). The signature of the ionic current is therefore of paramount importance in the experiments, as it carries the signature of the polymeric molecule passing through the pore.

The full details of the current blockade phenomenon are extremely complex: the involved variables are the pore size, pore geometry, chemical associations and charge condensations on the pore, ionic conditions on both sides of the separating membrane (including the ionic cloud that may condense around the pore), concentration of the macromolecules in the solution, ionic condensation on the macromolecules, voltage difference across the pore and temperature. Some of these variables may not stay constant throughout the typical duration of an experiment [2, 3, 5]. Taking all these into account in detail (without some level of coarse-graining) to model translocation is beyond the present day capabilities of theory and computer simulations.

At a broader and more phenomenological level of classification for the above complexities, the translocation process can be viewed as controlled by four main factors: (i) external driving fields, (ii) polymer dynamics, (iii) properties of pores/channels, and (iv) polymer–pore interactions. In this review we provide a combined theory–experiment progress report on the understanding of (bio)polymer translocation. To this end we note that several review articles have already been published [2, 4, 6, 7, 19–28]. One group of reviews [4, 20, 21, 23, 24, 26] tilts heavily towards the experimental side and mostly biological nanopores are discussed, the second group [6, 7, 27, 28] focuses more on artificial nanopores as biosensing devices, the recent theoretical review [19] presents a more general theme of polymer dynamics within confinements with emphasis on computer simulations, while the book [2] concerns mostly with theoretical descriptions of the translocation process from a quasi-equilibrium and phenomenological angle. An opening therefore remains for reviewing the developments in (the non-equilibrium aspects of) polymer dynamics of translocation purely from the theoretical side, relatively unrelated to the experimental nuances. That is the main focus of this review. We do not treat the review as an encyclopedic narrative, listing the papers and then summarizing their results. Instead, we aim to provide a unified picture to the reader—how we perceive the different studies fitting together (or not); this means that we are forced to leave out papers that marginally contribute to this unified picture.

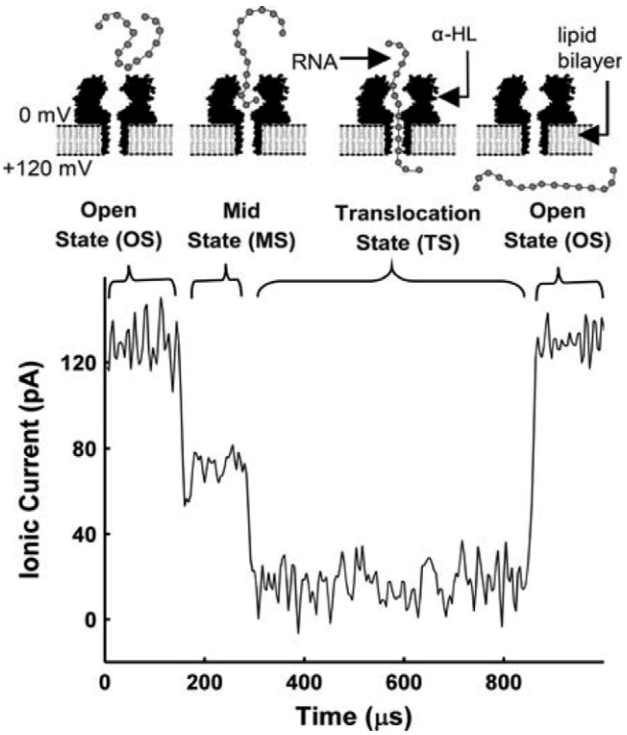

Figure 1. A schematic representation of a translocating RNA through an α-hemolysin pore embedded on a lipid bilayer membrane, showing that the blockade of the pore by the polymer coincides with the blockade of the ionic current. Since the α-hemolysin pore cross-section is not uniform, the current blockade characteristics depends on the details of the pore-blockade. Reproduced with permission from [18]. Copyright 2006 Elsevier.

We begin by a glossary in section 2. Thereafter, in order to remind the reader of the complexities associated with polymer translocation, we begin with a concise summary of the experimental developments in section 3. We then move on to a brief description of the main conceptual aspects of the translocation process in section 4. In section 5 we compare the different approaches to polymer dynamics of translocation. In section 6 we summarize the experimental aspects still in want of theoretical understanding. We finally end this review in section 7 with a brief discussion on where this field is likely to head to in the coming years.

2. Glossary

- *Persistence length.* A mechanical property of a polymer quantifying the distance over which it preserves its spatial

orientation, often denoted by the symbol l_p. Molecules much shorter than the persistence length resemble straight rods. The persistence length of long double-stranded DNA is typically ~50 nm (150 bp).

- *Pore or a channel?* A pore refers to the case when the membrane is thin, while a channel refers to the case of a thick membrane (i.e., a long pore). The pore or channel distinction depends on the comparison of membrane thickness t with persistence length l_p and aperture a. For $t \lesssim l_p$, or a, or both, it is translocation through a pore; otherwise, if $t \gg l_p$ and a, it is translocation through a channel. Unless otherwise stated, this review will consider translocation through a pore.
- *Debye length.* It is the length scale by which the mobile ions screen out the electric field. Its value depends on the electrolyte concentration used in the experiments, and rarely exceeds a few nanometers at typical experimental high-salt conditions. In addition, it is assumed that the electric field that typically drives translocation, is, for all practical purposes, confined only within the pore.
- *A translocation event, dwell time and translocation time.* A polymer makes many attempts to cross the pore; the unsuccessful attempts result in ionic current blockades of very short durations. Although during these times the pore is blocked by the polymer, these short blockages are not interesting, and are therefore digitally filtered out in experiments. A translocation event therefore coincides with pore-blockade across which the polymer crosses the pore. The compartment in which the polymer was before translocation is called *cis* (Latin for 'this'), whereas the one in which it is after translocation is called *trans* (Latin for 'across'). The time taken during a translocation event is synonymously defined in the literature as pore or current blockade time, and also known as the dwell time. One has to distinguish the dwell time and the translocation time (also known as the transit time) which is the average time for a polymer to navigate across the membrane.
- *Phantom and self-avoiding polymers.* A phantom polymer is allowed to intersect itself whereas a self-avoiding polymer is not. One result that will be used often in this review is that the radius of gyration R_g for a self-avoiding polymer of length N scales as N^ν, where ν is the Flory exponent; $\nu = 3/4$ and ≈ 0.588 in two and in three dimensions respectively. The radius of gyration for a phantom polymer of length N scales as $\sqrt{N}$.
- *Rouse and Zimm polymers.* Rouse proposed a model for polymer dynamics in 1953, in which hydrodynamic interactions among the monomers are completely screened [29]; it is known as the Rouse model. A key characteristic of this model is that the equilibration time for a polymer of length N scales as $N^{1+2\nu}$, where ν is the Flory exponent. In 1956, the model was extended by Zimm to include hydrodynamic interactions among the monomers [30] and the corresponding model is known as the Zimm model. The equilibration time for a polymer of length N in the Zimm model scales as $N^{3\nu}$.
- *Anomalous dynamics.* The dynamics of a particle is called anomalous if its mean-square displacement $\langle \Delta s^2(t) \rangle$ in time t scales as t^β for some $\beta \neq 1$; the case $\beta = 1$ denotes the 'normal' or Fickian diffusion.

3. A summary of the key experimental developments

3.1. External fields

It is entropically unfavorable for a polymer molecule to enter into the pore due to a significant decrease in number of degrees of freedom, leading to an entropic barrier [2] (in section 4 we will address this in detail). This entropic barrier is typically overcome by utilizing external electric fields since most macromolecules used in nanopore experiments are charged [31–33]. Experiments indicate that increasing the strength of the electric field decreases the translocation times exponentially. The external field can also be used to slow down the threading motion of the polymer molecules [34].

3.2. Polymer dynamics aspects

Originally, translocation experiments have involved only RNA and single-stranded DNA molecules moving through α-hemolysin biological pores [8, 18, 21, 35–45]. These molecules are very flexible and highly charged, which allows them to be driven through the pore by an applied electric field. The translocation events are associated with transient dips in ionic currents, and the length of these blockades is related to polymer lengths [4, 35, 38]. Analysis of blockade duration times and currents has indicated that nanopores can successfully discriminate between different types of polynucleotides [21, 36, 37], although a single-nucleotide resolution has not been achieved, mostly due to polymer fluctuations [21]. It has also been shown that nanopore translocation measurements might be used to evaluate the phosphorylation state, chemical heterogeneity as well as the orientation of entering nucleic acid molecules with a high sensitivity [8, 18, 42, 44]. Striking experiments from Meller's group [8] pointed out that it is possible to distinguish 3′ or 5′ end translocations of identical DNA molecules. This is because different packing and orientation of individual DNA bases in the channel produce different effective interactions with the pore, leading to different dynamics that can be observed in nanopore translocation experiments.

The high sensitivity of nanopore translocations has been utilized later in creating a single-molecule method for analyzing the dynamics of processes associated or coupled to DNA and RNA molecules such as unzipping kinetics of double-stranded DNA molecules and hairpins [39, 40, 43, 46], DNA–protein interactions [47, 50], helix–coil transitions [45] and processive replication of DNA by polymerase enzymes [11, 12]. These experiments have also led to a development of a new single-molecule dynamic force-spectroscopy method [43, 47–49], similar to existing AFM methods, although with much higher resolution, sensitivity and robustness that has turned out to be extremely important for investigations of various biological systems.

The success of translocation experiments for studying DNA and RNA molecules and related processes have stimulated significant efforts to utilize this approach to investigate other biological [51, 52, 55–58] and synthetic polymers [59–63]. Protein translocations are critically important for successful functioning of all biological systems since more than 50% of proteins produced in cells must traverse cellular membranes [1, 2]. Experimental measurements of transport of polypeptides molecules via α-hemolysin channels indicate that the overall translocation process can be described by a simplified two-barrier single-well free energy profile that strongly depends on the strength of the external electric field and on the length of peptide molecules [51, 56–58]. Nanopores have also been used to analyze the structure of peptide molecules in the case of collagen related systems where some intermediate conformations have been observed [52]. In addition, the nanopore recording technique was useful for studying protein folding dynamics with good sensitivity and controlled spatial resolution [55]. For non-biological polymers several studies concentrated on the use of flexible polyethylene glycol molecules [59–61] for understanding polymer partitioning in nanopores. Although these experimental results suggested that the partitioning follows a simple scaling law of de Gennes, other experiments [59] and theory [53, 54] suggest that there ought to be deviations from this scaling law. In another study [63], the translocation of dextran sulfate molecules has been utilized for investigating the effect of screening in the transport of polyelectrolyte molecules. Additionally, the nanopore threading of another synthetic polyelectrolyte, sodium poly(styrene sulfonate), has been analyzed as a new way of controlling the transport of macromolecules for future nanotechnological applications [62].

3.3. Properties of nanopores

The central part of all translocation processes is a pore that provides a confined space for polymer motion. Physical and chemical properties of channels play a critical role in the success of nanopore experiments [2]. There are two types of nanopore devices currently used in studies of polymer transport across the channels. One of them is based on the biological toxin protein α-hemolysin that inserts spontaneously into membranes, forming roughly cylindrical pores with a diameter of $\sim$1.5 nm in the narrowest part [4, 8, 12, 18, 21, 35–44, 51, 56–64]. This channel is always in the open configuration, allowing small molecules, ions and polymers to go through the membrane. The advantage of using this biological pore is the fact that it can be chemically modified via mutations to study different aspects of polymer translocation [2, 4, 51, 56–58]. In experiments performed by Movileanu and co-workers [51, 56–58] it has been shown that mutations introducing negatively charged acidic binding sites at special positions of the nanopore might significantly facilitate the transport of cationic polypeptides. In addition, utilization of this protein channel is advantageous for studying biologically oriented problems of polymer translocation. The biological nature of the α-hemolysin channel has been successfully utilized for the observation and explicit measurement of helix–coil transitions in some polynucleotide molecules [45]. However, there are also many problems associated with applications of biological nanopores, such as restricted sizes and limited stability with respect to the changes in external physical and chemical parameters [7, 65]. It is worthwhile to note that recently other membrane proteins have also been utilized as channels for polymer translocation [66–69].

Stimulated by shortcomings of biological channels, another approach that utilizes artificial nanopores in solid-state membranes has been proposed [6–8, 10, 11, 65, 70–86]. Solid-state nanopores provide a controllable and reproducible method of investigation of polymer threading at different conditions that can also be easily connected with other single-molecule methods [7, 74, 76, 85]. Polymer translocations through artificial nanopores have been successfully coupled with optical-trap devices that allowed explicit measurement of forces that drive charged macromolecules through confined regions [74, 76]. It has also been observed that polymer threading through solid-state channels made from silicon nitride and related materials might differ from the dynamics observed in biological channels [72]. These experiments show that translocation times of a double-stranded DNA through $\sim$10 nm pores have a power-law dependence as a function of the DNA length, in contrast to a linear dependence observed in the α-hemolysin channel. In another set of experiments on solid-state artificial nanopores, it has been illustrated that double-stranded DNA molecules can pass the channel in many conformations including linear and folded states [71]. Recently it has been shown that solid-state nanopores can be fabricated from non-silicon materials. Several experimental studies have indicated that single-walled carbon nanotubes can serve as channels for translocation of single-stranded DNA molecules [10, 87]. In addition, a new exciting possibility for pore transport came with a discovery of graphene: it was suggested recently that graphene nanopores can be viewed as perfect ultra-thin pores for polymer translocation [86, 88–91]. Another interesting direction for new nanopore devices has been proposed recently with the development of opal films [92]. However, although the application of artificial channels had many successes in various scientific fields, synthesized pores also have several serious disadvantages due to the inability to create reliable nanopores with small diameters, and complex chemical interactions with translocating polymers created by the fabrication procedures [8, 78, 85]. It is important to take into account different properties of biological and artificial nanopores in order to understand fundamental properties of polymer translocation.

3.4. Polymer–pore interactions

Nanopore experiments directly measure the pore-blockade time, which is strongly affected by these interactions [2, 8, 14, 93]. Mirsaidov *et al* have shown that it is possible to discriminate DNA with and without covalent methylation modifications of cytosines [93]. Using a synthetic biconical

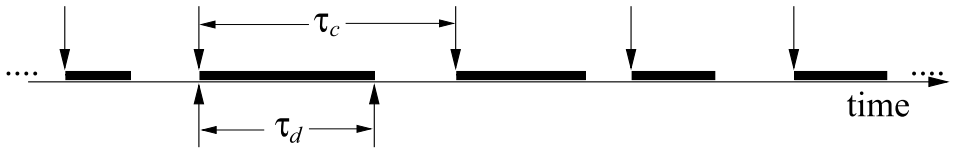

Figure 2. A schematic representation of the translocation process, where only the pore blockades during translocation events are shown by thick bars. The captures are indicated by a black downward arrow. See text for the definition of capture. Relative magnitudes of pore-blockade time τ_d and capture time τ_c has been made out of scale in order to provide visual clarity. The figure provides an abstract version of figure 1.

nanopore the permeability of different DNA molecules has been measured with high precision, suggesting the critical role of polymer–pore interactions. Using tethered oligonucleotides Howorka and Bayley [94] have determined the electric potential within protein pores, supporting the idea that the main potential drop is taking place across the β-barrel of the α-hemolysin channel. The sensitivity of nanopore experimental methods for polymer–pore interactions have been also demonstrated in striking experiments on single-stranded $3'$ and $5'$ end DNA translocations [14]. Based on pore–polymer interactions, nanopore techniques as a new mass-spectroscopic method for separation of macromolecules has also been proposed and successfully utilized [95–97].

4. Generic description of the translocation process

4.1. Translocation is an activated process

A key generic property revealed by many of the experiments is that translocation is an activated process. The activation barrier is of entropic origin: the polymer enjoys many more configurational possibilities in the bulk—far away from the membrane (where the pore/channel is embedded)—than when it is threaded through the pore. The height of the barrier, therefore, can be theoretically estimated as follows. For a self-avoiding polymer of length N, the number of configurational states per volume, accessible to it in the bulk scales as $Z_b(N) \approx A\mu^N N^{\gamma-1}$ in which γ is a universal exponent—$\gamma = 49/32$ and $\gamma \approx 1.16$ in two and three dimensions respectively—while A and μ are not universal [98]. The corresponding number of states per volume for the same polymer, but whose one end has just about reached the pore, and therefore can be thought of as tethered to the membrane, is approximated by $Z_w(N) \approx A_1\mu^N N^{\gamma_1-1}$ in which the parameter μ is not affected by the introduction of the membrane, γ_1 is a different universal exponent—$\gamma_1 = 61/64$ and $\gamma_1 \approx 0.68$ in two and three dimensions, respectively—while A_1 is again not universal [98]. Now consider the translocating polymer, for which there are n monomers on one side and $N-n$ monomers on the other (assuming that the nanopore is ultra-thin so that there are no monomers inside the channel). Since this situation can be seen as two strands of polymers with one end (of each strand) tethered on the membrane, the number of states for this polymer is given by $Z_w(n)Z_w(N-n)$, which attains a minimum when $n = N/2$. The entropic barrier faced by a translocating polymer is thus

$$\Delta S = \log \frac{Z_b(N)}{Z_w^2(N/2)} = c \log N + k, \qquad (1)$$

with $c = \gamma - 2\gamma_1 + 1$ and $k = \log A - 2\log A_1 + 2(\gamma_1 - 1)\log 2$.

4.2. The three stages of translocation dynamics

The entropic barrier, obtained above from the partition function is an equilibrium property. It states that when an ensemble of polymers is placed in two chambers A and B that are separated by a membrane and are connected only by a narrow pore, the ratio of the probabilities of finding a polymer of length N far away from the membrane and being threaded through the pore with n monomers in one chamber and $(N-n)$ in the other is given by $Z_b(N)/[Z_w(n)Z_w(N-n)]$. Translated to the case of a single translocating polymer in chamber A, and not an ensemble of them, it means that the polymer, on its way to chamber B, will turn back many times to chamber A before it actually succeeds in translocating. This divides translocation dynamics into three distinct stages that take place in succession: (i) approach of the polymer in the vicinity of the pore, followed by repeated threading and unthreading of one of its ends into the pore, (ii) a final threading into the pore, which is often referred to as 'capture' in the experimental literature, and (iii) the eventual translocation event. Every time there is a threading event, the polymer occupies a substantial cross-section of the pore, blocking the ionic current, although only for short durations. A translocation event corresponds to the blockade of the ionic current as well, but for longer times. The long(er) ionic current blockade is therefore preceded by many short(er) spikes of ionic current blockade events caused by repeated threading and unthreading events, and are digitally filtered out in experiments. A sequence of such filtered out current blockade events is schematically shown in figure 2. When the sequence of current blockade events is followed over a long time, one can obtain sufficient statistics of the process, from which an average capture time τ_c (or equivalently the capture rate τ_c^{-1}), and the average pore-blockade time τ_d can be obtained.

Below we briefly describe the main issues related to the capture process.

4.3. The capture process

4.3.1. Dependence of the capture rate on macromolecular concentration c. At the low density of macromolecules used

in experiments, the rate limiting step in translocation is the availability of the macromolecules in the immediate vicinity of the pore. Given that the macromolecules disappear from the *cis*-side of the pore, one should think of the pore as a sink for the macromolecules. Although there is a voltage across the pore, under typical experimental conditions the Debye length barely exceeds a nanometer, and the effect of the field is highly localized in the pore. In such a situation, a steady state in the macromolecular concentration profile exists on the *cis*-side: at the pore, because of the presence of the sink the macromolecular concentration is lower, while far away from the pore the number density is given by c. This sets a gradient of macromolecular concentration on the *cis*-side, and generates a drift of macromolecules towards the sink. The macromolecular current density $\vec{J}$ must be proportional to the concentration gradient.

Since the density of macromolecules in experiments is low, these hardly encounter each other. Thus, all processes, in particular the capture and translocation processes, will occur with rates that scale linearly with the overall concentration c: if there are twice as many macromolecules, the total concentration profile will simply scale up by a factor 2, and as a result twice as many macromolecules will reach the pore and succeed in translocation.

4.3.2. Dependence of the capture rate on other parameters. Given that the capture rate τ_c^{-1} is also the throughput rate for translocation, several experiments have studied the capture phenomenon using both biological pores such as α-hemolysin as well as synthetic pores [8, 31, 32, 55, 85, 99]. These reveal four key characteristic properties of the capture rate.

(i) It is proportional to the macromolecular volume concentration in the buffer solution [8, 31, 32, 55, 85, 99]. Typical concentrations of macromolecules used in these experiments are a few μg ml^{-1}. At these concentrations molecules do not interact with each other, and the rate-limiting step for the throughput of a translocation experiment is the capture process, as $\tau_d \ll \tau_c$.

(ii) It depends exponentially on the bias voltage V applied across the pore above a threshold value; i.e., there is an activation barrier for the capture process [8, 32, 55, 85]. E.g., in [32] poly(dC)$_{40}$ was translocated through α-hemolysin pores in a 1M KCl buffer, and data for τ_c versus V demonstrate the existence of two different activation barriers at low and high values of V, with a sharp crossover at approximately 130 mV. In a more recent study [85], for the translocation of λ-phage DNA through synthetic SiN nanopores in the same buffer a single exponential was reported for smaller molecules, but for longer DNA molecules the relation between the capture rate and V was found to be linear (although the data for longer DNA molecules can also be fitted with an exponential).

(iii) The length dependence of the capture rate is far less clear. Stretched exponential behavior of the capture rate up to a certain length of the polymer (and length-independent behavior thereafter) has been reported in [85]. At present, there is no theoretical understanding of this behavior.

(iv) The capture rate is dramatically influenced by the application of a salt gradient across the pore: a higher (lower) salt concentration on the *trans*-side enhances (reduces) the capture rate. E.g., in the experiments of [85], a 20-fold increase in the KCl concentration on the *trans*-side of the membrane increased the capture rate by almost a factor of 30. Although this enhancement was originally thought to be due to electro-osmotic flow, it has recently been established that the enhancement is caused by pure osmotic flow (of water) from the low-salt concentration side to the high-salt concentration side [100]. The DNA is simply dragged along the water flow, much like logs floating along a stream.

(v) Another surprising feature of the capture process reported in [99] is the observation of a capture radius $\sim$3 μm around the pore. The experiments are performed with synthetic silicon nitride nanopores and 16.5 μm long λ-DNA. The existence of the capture radius around the pore—which means that once a DNA molecule entered this volume, it did not escape during the time of experiment—was observed using fluorescence spectroscopy. The electro-osmotic flow has been posited to explain this phenomenon [101].

For this explanation however, the macromolecule was considered to be a point mass located at its center of mass, and therefore was not considered to be an extended object. Indeed, if the DNA is considered to be an extended object, then a back-of-the-envelope calculation—even with the assumption that it is not stretched or deformed close to the pore at the micron scale—it is possible to argue that the capture radius should be in the range of 2 μm, and the fluorescent spectroscopy images are not precise enough to be able to resolve differences between 2 and 3 μm. E.g., at 16.5 μm length, and with persistence length $l_p = 33$ nm, the DNA in the experiment [99] consisted of $N = 500$ persistence length segments. For a polymer chain whose conformation obeys Gaussian statistics, the end-to-end length is $\sim l_p\sqrt{2N} \approx 1$ μm. However, the DNA is not described by Gaussian statistics, but by self-avoiding polymer statistics; assuming that the conversion prefactor between Gaussian and self-avoiding prefactor is $\approx$1, the end-to-end length of the DNA is $\sim l_p(2N)^\nu \approx 1.8$ μm, where ν is the Flory exponent of the polymer $\approx$0.588 in three dimensions. Further, since we expect the capture process to be dominated by fluctuations (i.e., the polymer finds the pore by fluctuations), one needs to consider the statistics of the furthest points of a polymer chain, and not simply the end-to-end extent in space. This brings another factor of 1.2, implying that one can expect the capture to take place when the macromolecule's ends are about $1.2 l_p N^\nu/\sqrt{2N} \approx 2.2$ μm apart from each other. This number is close enough to the value $\sim$3 μm for the capture radius, observed through fluorescence spectroscopy.

One implication of this alternative explanation is that one would observe a higher capture radius for longer macromolecules. However, at the time of writing this

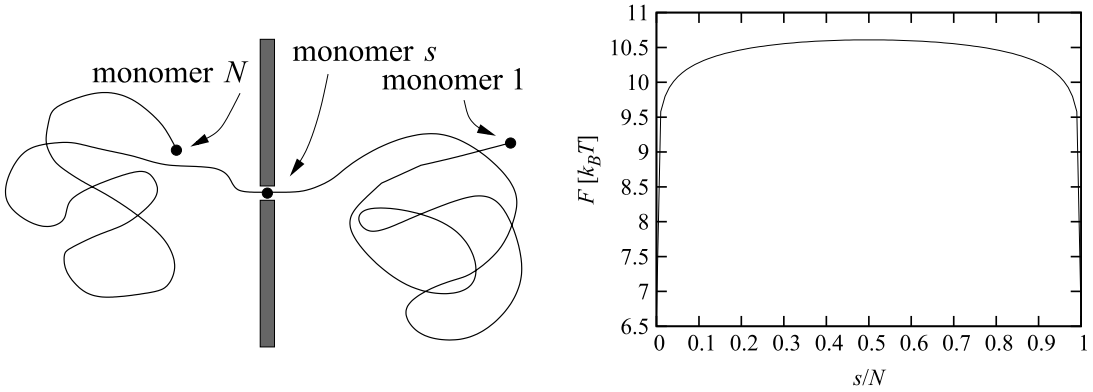

Figure 3. Left: snapshot of a translocating polymer in a two-dimensional projection. The reaction co-ordinate $s(t)$ denotes the monomer index located at the pore at time t. Right: the entropic barrier as a function of the reaction co-ordinate s/N for $N = 10^6$. Note that, apart from the first and last ∼1%, the free energy is within k_BT of its maximal value.

review, we are not aware of any systematic study on the capture radius as a function of macromolecule length.

4.4. Entropic barrier and pore-blockade time for long polymers

As already discussed in section 4.1, at a single-polymer level the activation barrier manifests itself in repeated threading–unthreading events before the polymer actually manages to translocate. The pore-blockade time, which is obtained after these repeated threading–unthreading events are filtered out, is in fact independent of the entropic barrier [102]. The pore-blockade events are controlled by polymer dynamics, polymer–pore interactions, properties of nanopores and external fields. Of these, the last three have been well-covered in a recent book [2]; we therefore take up the issue of polymer dynamics and the pore-blockade time in detail in section 5.

5. Polymer dynamics and pore-blockade time

There exists a substantial body of literature, mostly due to theorists and simulators, who have been interested in translocation as a specific example of a wide family of related activated processes in statistical physics, including, for instance, nucleation theory. These studies are therefore largely disconnected from experimental considerations, unless they address generic aspects of translocation as an activated process. In this section we divide them into three categories: (i) unbiased translocation (translocation in the absence of external driving, i.e., purely by thermal fluctuations), (ii) field-driven translocation (translocation driven by a field essentially acting at the pore—the field can be of different origin, such as a physical electric field, an entropic force or a chemical potential gradient), (iii) translocation mediated by pulling the lead monomer by optical tweezers.

5.1. Unbiased translocation

To a large extent, the theoretical approach of pore-blockade from the polymer dynamics angle stemmed from the experimental paper by Kasianowicz *et al* [35]. The early models of a translocation event reduced polymer dynamics through the pore to the dynamics of $s(t)$, the index of the monomer located in the pore at time t. For a polymer consisting of N monomers, by definition, $s(0) = 1$ and $s(\tau_d) = N$. Borrowed from chemical physics parlance, the quantity $s(t)$ (see figure 3) is termed as the 'reaction co-ordinate'. The introduction of this quantity allowed the early researchers to compute the configurational entropy of the chain as a function of $s(t)$ (concept described in section 4.1), rendering translocation events simply to the motion of an effective single particle, located at $s(t)$ at time t, over an entropic barrier.

5.1.1. Early works on pore-blockade as a quasi-equilibrium process. Aside from the fact that treating translocation as an entropic barrier crossing process does not filter out the repeated threading–unthreading sequences that precede the translocation event, there is another note of caution that needs to be spelled out for this approach. Since entropy is an equilibrium concept, applying the entropic barrier concept to study pore-blockade in these early theories on unbiased translocation [103, 104] assumes that at every stage of translocation the polymer has the time to thermodynamically explore its entire space of configurations, and therefore the polymer dynamics through the pore is a quasi-equilibrium process. In any case, from the forms of the partition functions discussed in section 4.1, it is clear that the height of the entropic barrier as a function of the reaction co-ordinate s is of the form $\log[s(N - s)]$ (in [103, 104] only phantom polymers were considered, and not self-avoiding polymers, but the form remains the same), and therefore the barrier is essentially flat around $s = N/2$ in the scaling limit (polymer length $N \to \infty$). The effective particle then has no drive to move either way on this flat part of the barrier, which stretches for a length of order-N in the scaling limit, and as a consequence, its motion is diffusive. The time taken by this effective particle to cross the barrier—the pore-blockade time for a translocation event—therefore scales as N^2/D, where D is the effective diffusion coefficient of the particle on this entropic landscape.

In [103] the authors assumed that D is a function of N, and used $D \sim N^{-1}$ for phantom Rouse polymers,

leading to $\tau_d \sim N^\alpha$ with $\alpha = 3$. Correspondingly, for phantom Zimm polymers, $D \sim N^{-1/2}$ was used, which led to $\tau_d \sim N^\alpha$ with $\alpha = 5/2$. (Strictly speaking, this time is not the true pore-blockade time as it includes the repeated threading–unthreading times as well, but in the scaling limit the latter might be negligible.) Muthukumar [104] subsequently corrected these results arguing that D should be independent of N, which led to the scaling exponent $\alpha = 2$. Slonkina *et al* later generalized these results to channels [105].

As it turns out, the quasi-equilibrium approximation is a drastic simplification as far as scaling results are concerned. We will discuss its applicability in section 5.1.3, and discuss its predictions for field-driven translocation in section 5.2.2.

5.1.2. Pore-blockade as a non-equilibrium process and anomalous polymer dynamics. That the quasi-equilibrium approximation does not hold in the scaling limit was first pointed out by Chuang *et al* [106]. They argued that in order to be able to use the quasi-equilibrium approximation, the polymer needs to have sufficient time to explore all the accessible configurational states at every value of the reaction co-ordinate. As the characteristic time for the polymer tails on the *cis*- and *trans*-side increases with polymer length, the quasi-equilibrium approximation has to break down at some point. They illustrated this point by considering translocation of a self-avoiding Rouse polymer: its equilibration time scales as $N^{1+2\nu}$, which, in the scaling limit will always be far greater than the scaling of the pore-blockade time $\tau_d \sim N^2$ predicted by the quasi-equilibrium approximation.

Chuang *et al* [106] further argued for a lower limit for the scaling of the pore-blockade time τ_d for a Rouse polymer, as follows. After a translocation event, the polymer displaces itself by its radius of gyration, which scales as N^ν for a self-avoiding polymer of length N. If the pore width is infinite (i.e., there is no membrane separating the *cis* and the *trans* sides), then the polymer crosses the pore simply by diffusion, and the time scale for crossing the pore follows the well-known Rouse scaling $N^{1+2\nu}$. When the pore is narrow, allowing the monomers to pass through only sequentially, the pore-blockade time can only be larger. They followed up this argument by computer simulation using the bond-fluctuation model [107] (BFM—a model for self-avoiding Rouse polymer dynamics), and found that the lower limit $N^{1+2\nu}$ for the scaling of τ_d is saturated. The result meant that the dynamics during a translocation event is anomalous: if the mean-square displacement $\langle \Delta s^2(t) \rangle$ of the reaction co-ordinate in time has to scale as t^β for some β, the condition $\langle \Delta s^2(\tau_d) \rangle = N^2$ along with $\tau_d \sim N^{1+2\nu}$ means that $\beta = 2/(1 + 2\nu)$ (i.e., $\beta \neq 1$) [106]. Their work was quickly followed by an incredible body of literature to test these exponents, leading to, what is colloquially known to researchers in this field, 'an exponent war'.

For a number of years following the work by Chuang *et al* [106], several simulation studies, using BFM, bead–spring molecular dynamics (MD) and GROMACS, reported the value of α both in 2D and 3D to be consistent with $1 + 2\nu$ (which equals 2.5 in 2D, and $\approx$2.18 in 3D [108–110]). Some of these studies characterized the anomalous dynamics of unbiased translocation as well: the mean-square displacement of the monomers $\langle \Delta s^2(t) \rangle$ through the pore in time t was found to scale $\sim t^\beta$ with $\beta = 2/(1 + 2\nu)$, satisfying the obvious requirement $\langle \Delta s^2(\tau_d) \rangle = N^2$. However, several other subsequent/concurrent theoretical and simulation studies—simulations using finitely extensible nonlinear elastic (FENE) model [123], MD and dissipative particle dynamics (DPD) for modeling hydrodynamic interaction among the monomers [124]—later found that α and β for a Rouse polymer significantly differed from $1 + 2\nu$ and $2/(1 + 2\nu)$ respectively [102, 113–122]. The latter results on the pore-blockade time exponent concentrated around $2+\nu$ for Rouse, and $1 + 2\nu$ for Zimm polymers. All these results are summarized in table 1.

Given that the predictions/confirmations of $\alpha = 1 + 2\nu$ for Rouse polymer came solely from simulations without a theoretical basis behind it, while there is a theory that obtains $\beta = (1 + \nu)/(1 + 2\nu)$, and correspondingly, $\alpha = 2 + \nu$, we spend a few sentences on the latter result. It was originally obtained by two of us [113–115, 125] using a theoretical approach based on polymer's memory effects that stem from their local (in the vicinity of the pore) strain relaxation properties, and it was further tested by simulations with a highly efficient lattice polymer model. The strain results from the motion of monomers across the pore: as a monomer hops from the left to the right of the pore, the polymer locally stretches on the left and compresses on the right, giving rise to a local strain, in the form of chain tension imbalance, across the pore. This imbalance can relax via two different routes: (i) instantaneously, if the hopped monomer hops back, and (ii) along the polymer's backbone on both sides of the membrane, which requires a finite time (the time is simply the Rouse equilibration time $\tau_R \sim N^{1+2\nu}$, which is the time scale for the memory of the chain tension to survive). Until this time the hopped monomer has an enhanced chance to hop back. When properly worked out [113–115, 125], the memory decays in time as a power-law, as $t^{-(1+\nu)/(1+2\nu)}$. This leads to $\langle \Delta s^2(t) \rangle \sim t^{(1+\nu)/(1+2\nu)}$ (i.e., $\beta = (1 + \nu)/(1 + 2\nu)$) up to τ_R, and thereafter as Fickian diffusion, $\langle \Delta s^2(t) \rangle \sim t$ (i.e., $\beta = 1$). These further lead to $\alpha = 2 + \nu$ ($\approx$2.588 in 3D and 2.75 in 2D) [113–115]. For a Zimm polymer, the memory effects similarly predict $\langle \Delta s^2(t) \rangle \sim t^{(1+\nu)/(3\nu)}$ up to the Zimm equilibration time $\tau_Z \sim N^{3\nu}$, and thereafter $\langle \Delta s^2(t) \rangle \sim t$; leading to the expectation that τ_d should scale as $N^{1+2\nu}$ [113, 114]. (The fact that $\alpha = 1 + 2\nu$ for a Zimm polymer has nothing to do with Rouse dynamics. It is in fact a pure coincidence that this exponent is the same as that of τ_R [113, 114].)

Before we discuss how the apparent differences in the values of α are reconciled, it would be worthwhile to make a note here on the attempts to classify the anomalous dynamics of translocation. It was proposed originally in [126] that anomalous dynamics of translocation can be expressed in terms of fractional Fokker–Planck equation, which is based on the continuous time random walk (CTRW) formalism. Subsequently, some researchers have followed this route [116, 127, 128]. The memory effect description for anomalous dynamics of polymer translocation, on the other hand,

Table 1. Summary of all the results on the exponent for the pore-blockade time for unbiased translocation known to us at the time of writing this review. Abbreviations are explained in main text.

References	α (2D, Rouse)	α (2D, Zimm)	α (3D, Rouse)	α (3D, Zimm)
[106]	$1 + 2\nu = 2.5$	—	—	—
[108]	(BFM)			
	2.50 ± 0.01 (BFM)	—	—	—
[109]	2.48 ± 0.07	—	—	—
	(FENE MD)			
[110]	2.51 ± 0.03	—	2.2	—
	(bead–spring MD)		(bead–spring MD)	
[111]	2.5 (BFM)	—	—	—
[112]	2.44 ± 0.03	—	2.22 ± 0.06	—
	(GROMACS)	—	(GROMACS)	—
[113, 114]	—	—	$2 + \nu \approx 2.588$	$1 + 2\nu \approx 2.18$
[115]	$2 + \nu = 2.75$	$1 + 2\nu = 2.5$	—	—
[116]	—	—	2.52 ± 0.04	—
			(FENE)	
[117]	—	—	$2 + \nu$	$1 + 2\nu$
[118]	—	—	—	2.27 (MD)
[119]	—	—	—	$11/5 = 2.2$ (MD)
[120]	—	—	—	2.24 ± 0.03 (DPD)
[121]	—	—	2.516 (FENE)	
[122]	—	—	2.52 (FENE)	

belongs to a general framework of ubiquitous examples of anomalous dynamics in polymeric systems, based on the generalized Langevin equation (GLE) [129, 130]. The GLE formulation also establishes that the anomalous dynamics of translocation belongs to the class of fractional Brownian motion (fBm) [111, 131, 132]. Given that fBm and CTRW are mutually exclusive, the description of polymer translocation using the fractional Fokker–Planck equation is discredited by these studies.

5.1.3. Consensus on the value of α? How can the 'exponent war' finally end in a truce? Despite demonstrating that BFM is a pathological model for polymer translocation [133], the apparent dispute about the value of α was left alive and kicking. Recent work by de Haan and Slater [134] has finally shed an interesting light on this issue. They used the FENE model to simulate unbiased polymer translocation in three dimensions with varying viscosity $\tilde{\eta}$ of the surrounding medium. The results are spectacularly consistent with the memory function approach [113–115, 125]. At $\tilde{\eta} = 0$ they found $\alpha = 2$ corresponding to Fickian diffusion for the dynamics of polymer translocation—this is only to be expected since the tension imbalance in the vicinity of the pore then relaxes through the polymer's tails instantaneously, resulting in complete loss of the memory effects. As the viscosity is increased, the apparent exponent α increases, crossing $1 + 2\nu$, and at the highest value of viscosity used the apparent exponent α reaches $\approx$2.55 (runs with higher viscosity were not possible because of the prohibitive cost of computation [135]). There is a strong indication from the trend of the data that at very high viscosity the data would indeed correspond to $\alpha = 2 + \nu$, consistent with the prediction of the memory function approach.

Furthermore, de Haan and Slater [134] showed that if data from simulations with different viscosities and polymer lengths are combined, a data collapse can be obtained if τ_d/N^2 is plotted as a function of $\tilde{\eta}N^x$ with $x = 0.516$. In the limit of high viscosity, the translocation time is expected to increase linearly with viscosity. The data collapse at high viscosities predicts $\tau/N^2 \sim \tilde{\eta}N^x$, hence $\alpha = 2.516$, close to the theoretically predicted value $2 + \nu$.

In other words, the work by de Haan and Slater [134] shows that the true values of α are (i) 2 at zero viscosity and (ii) likely $2 + \nu$ at very high viscosity of the surrounding medium. The rest of the values reported in the literature are all apparent exponents. The corresponding figures by de Haan and Slater are reproduced in figure 4. As shown therein, curiously, choosing $\tilde{\eta} = 1$ in the model produces (the apparent exponent) $\alpha = 1 + 2\nu$ (the other arrow at $\tilde{\eta} = 5$ indicates the results of another study by the authors).

5.2. (Electric) field-driven translocation

The extension from unbiased translocation to (electric) field-driven translocation is in principle trivial: one simply adds a force on the monomers equaling the charge of the monomers (the charge per monomer is henceforth understood to be unity without any loss of generality) times the strength of the electric field E, acting from the *cis* to the *trans* direction. As explained in section 4, this is a reasonably accurate approximation since the electric field dies off rapidly within the Debye length, which is less than a nanometer under typical experimental conditions. However, as we will soon see, the presence of the electric field complicates the scaling issues.

5.2.1. Extension of the quasi-equilibrium picture. When such a field is added to the equation of motion in the quasi-equilibrium description of translocation, the entropic barrier, in terms of the reaction co-ordinate s, gets an overall linear tilt from the *cis* towards the *trans* side (figure 5). The result of this exercise is that on top of the diffusive

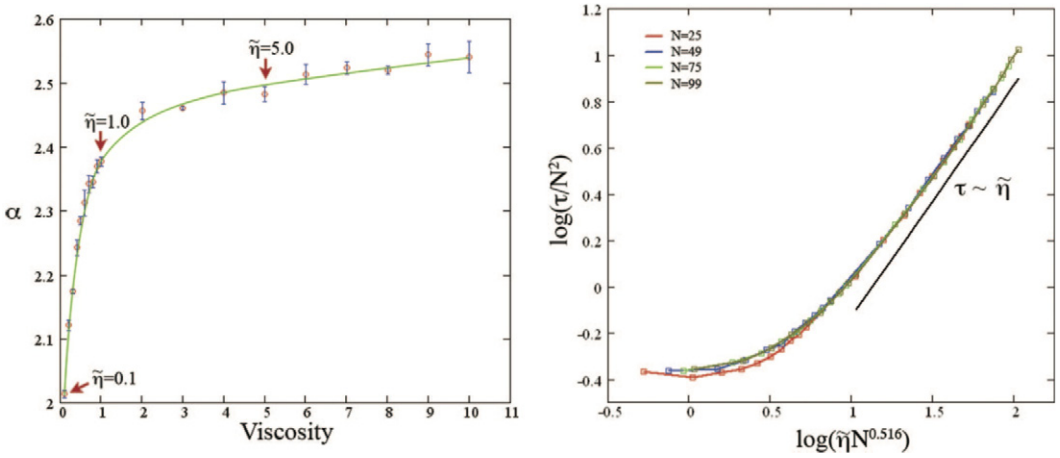

Figure 4. Results of a FENE simulation model for Rouse polymer translocation in three dimensions by de Haan and Slater. Left: the apparent pore-blockade time exponent α. Right: data collapse for τ_d/N^2 as a function of $\tilde{\eta}N^{0.516}$. Reproduced with permission from [134]. Copyright 2012 the American Institute of Physics.

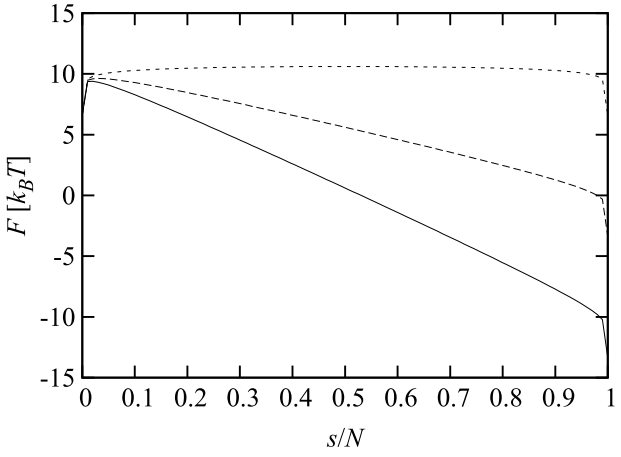

Figure 5. The tilted entropic barrier as a function of the reaction co-ordinate s/N in the presence of a small driving field for $N = 10^6$ (the values used for the field are 0.25 and 0.5 μeV per monomer respectively; higher tilt corresponds to stronger field). The no-tilt case is shown as a reference in small dashed line when there is no field acting in the pore (i.e., unbiased translocation). The tilt gets stronger with increasing field strength.

motion as described in section 5.1.1, the effective particle also has a constant drift towards the *trans* side, meaning that it traverses the entire length N of the entropic barrier with a uniform velocity, which is proportional to the field strength. Consequently, the pore-blockade time simply scales as N and is inversely proportional to the field strength [104, 105, 136].

It is to be noted that for the above to work *per se*, one does not need to have an electric field acting on the monomer straddling the pore. The field can have multiple origins, such as entropic due to (preferential) confinement [17, 137, 138] or adsorption to the membrane on the *trans* side [139]; in these cases the field E acting on each monomer in the pore for field-driven translocation is simply replaced by the chemical potential gradient $\Delta\mu$ for monomer transfer from the *cis* to the *trans* side, and we will summarily refer to all these situations as field-driven translocation.

5.2.2. Pore-blockade as a non-equilibrium process. Just like in the case of unbiased translocation, that the quasi-equilibrium picture cannot hold in the scaling limit was first pointed out by Kantor and Kardar [140]. They considered the case of a self-avoiding Rouse polymer driven by a field acting within the pore and argued that the pore-blockade time has a lower limit which scales as $N^{1+\nu}$, as follows. Consider a pore of infinite diameter, i.e., the motion of a free polymer of length N, of which one of the monomers is being pulled by a force E. The motion of the center of mass of this polymer is determined by the total force acting on the polymer, and thus results in a uniform velocity $\propto E/N$. When the polymer translocates, completely it displaces its center of mass by a distance that scales as its radius of gyration N^{ν}, i.e., the total time of translocation then scales as $N^{1+\nu}/E$. When the pore is narrow—for which the field acts on the monomer instantaneously located within the pore, but that is a matter of detail—the pore-blockade time cannot be less than the case when the pore is infinitely wide, leading to the lower limit for the pore-blockade time for translocation as $N^{1+\nu}/E$. They carried out simulations with the BFM in two dimensions, and concluded that this lower limit is saturated, i.e., $\langle\tau_d\rangle \sim N^{1+\nu}/E$.

Again, this study was followed by a rather large number of follow-up studies to confirm the result, and led to another exponent war, only messier. As we shall shortly see, this has to do with the fact that the addition of a driving field into the problem introduces an extra level of complication; however, the reported values of the exponent all fall in a consistent line once the scaling limit ($N \to \infty$) is properly interpreted in relation to E.

Rather than providing a chronological narrative for the values of α as reported by different research groups, we opt to first present the theoretical perspective as followed by Sakaue and co-workers, as we feel that this is the most robust description. A schematic representation of this process is shown in figure 6: for $E > k_BT/R_g$ they identified that the polymer on the *cis* side is composed of two domains, a moving one (moving with velocity $V(t)$; the range of this

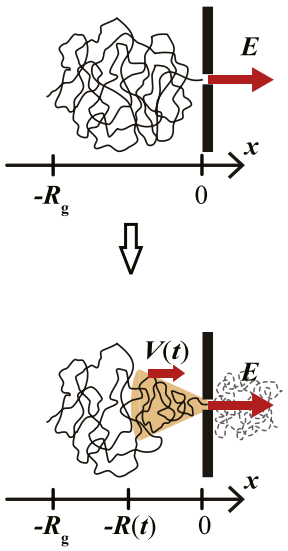

Figure 6. Schematic figure illustrating the 'tension propagation theory' by Sakaue and co-workers. We thank T Saito for providing us with this figure.

domain extends up to a distance $R(t)$ from the pore on the *cis* side, as shown in figure 6 with a colored background), and a quiescent one (beyond distance $R(t)$ from the pore); and the key to field-driven translocation dynamics is the shifting boundary between the two domains of the polymer, located at a distance $R(t)$ from the pore on the *cis* side, as it determines how the driving field is transmitted along the backbone [141–145]. The moving domain corresponds to a velocity and force–extension relation dictated by those of a polymer in the 'trumpet regime', while the quiescent domain corresponds to those of a polymer essentially unperturbed by the applied field. Matching the boundary conditions between the two domains then leads to the behavior of $R(t)$ as a function of t, and subsequently the pore-blockade time is determined from the relation $R(\tau_d) = R_g \sim N^\nu$. In other words, the pore-blockade time is dominated by the tension propagation time along the backbone of the chain. In this way α is shown to be equal to $1 + \nu$, although the exponent for the field-dependence of the pore-blockade time depends on the field strength, i.e., whether $k_BT/R_g < E < k_BT/a$ or $E > k_BT/a$, where a is the length of a monomer.

The same exponent has been obtained theoretically by Rowghanian and Grosberg [146] and Dubbeldam *et al* [147], using 'iso-flux trumpet' models. These models entail small variations of those of Sakaue and co-workers, and posit that instead of the polymer attaining the shape of a trumpet on the *cis* side, one should imagine a space-fixed trumpet, expanding in radius away from the pore on the *cis* side, and the polymer has to funnel through this trumpet. At any given time, the flux of monomers is uniform across any cross-section of the trumpet.

All these models presuppose that under the influence of the field the polymer takes a far-out-of-equilibrium shape; this assumption obviously has to break down if the field becomes small enough. At small enough fields the translocation dynamics can be simply extended as a linear response on the unbiased case, for which the memory function approach has done well, by adding a force on the monomer straddling the pore. The result is that in three dimensions, the pore-blockade time exponent α for weak fields is obtained from the exponent for the memory function, namely that $\alpha = (1+2\nu)/(1+\nu)$ for a Rouse polymer, and $= 3\nu/(1+\nu)$ for a Zimm polymer [148].

How can one distinguish weak and strong forces from each other? One assumption underlying the memory function approach applied to field-driven translocation is that the polymer's configurational statistics are not influenced by the applied field. A back-of-the-envelope calculation, analogous to the well-known coil to Pincus blob transition in polymer physics, leads to the result that the field strength satisfying the condition $E^*R_g = k_BT$ decides whether the field is weak or strong. This relation has recently been verified by Sakaue for the dynamics of a free polymer in bulk [149]. With $R_g \sim N^\nu$, this condition entails the following scenario: (i) for a Rouse polymer in two dimensions the pore-blockade time exponent is $2\nu = 1.5$ and $1 + \nu = 1.75$ for weak ($E < E^*$) and strong ($E > E^*$) fields respectively, and (ii) for a Rouse polymer in three dimensions the pore-blockade time exponent is $(1 + 2\nu)/(1+\nu) \approx 1.37$ and $1+\nu \approx 1.588$ for weak ($E < E^*$) and strong ($E > E^*$) fields respectively. Note that the crossover field strength E^* is decreasing with polymer length. Thus, no matter how small the field is, if the polymer gets long enough, the behavior will eventually cross over from the linear response regime to the regime described by Sakaue *et al*. This crossover was indeed argued (and shown numerically) by us in a related paper that mapped the dynamics of polymer adsorption to that of polymer translocation [150], wherein the adsorbing force (derived from the adsorbing energy) plays the role of the translocating force generated by the field. The argument rests on the assumption that at strong fields the polymer attains the so-called 'stem–flower' configuration [151], with a quiescent 'flower' consisting of the monomer cloud connected by a 'stem' of monomers to the adsorbing surface; the flux of monomers is brought to the adsorbing surface along the stem by the action of the adsorbing force.

For one, it is clear from the above discussion that the reported value of the pore-blockade time exponent has the potential to be easily influenced by the model parameters, in particular, how the scaling limit ($N \to \infty$) is interpreted in comparison to E (whether it is bigger or smaller than $E^* \sim N^{-\nu}$). In our view, this is the reason why establishing these exponents in simulations has been no trivial matter. A second source of complication is that Brownian and Langevin dynamics simulations very often introduce a pore friction, which also considerably influences the measured value of the exponent. Nevertheless, in tables 2 and 3 we report that there is quite some numerical support from the different research groups for $\alpha = 2\nu$ and $1 + \nu$ for a Rouse polymer in two dimensions, and $\alpha = (1 + 2\nu)/(1 + \nu)$ and $1 + \nu$ for a Rouse polymer in three dimensions[5].

[5] The list in tables 2 and 3 is by no means exhaustive. There are papers, such as [152–156], which report extensively on the effective pore-blockade time exponent as functions of simulation parameters, but we have found them difficult to interpret for including them in this review in a cogent manner.

Table 2. Summary of all the reported values of the exponent for the pore-blockade time for field-driven translocation of a Rouse polymer in two dimensions, known to us at the time of writing this review. Abbreviations: LD (Langevin dynamics), MC (Monte Carlo).

References	α (2D, Rouse)
[140]	$1 + \nu = 1.75$ (BFM)
[157]	1.46 ± 0.01 crossing over to 1.73 ± 0.02 with increasing N at fixed E (BFM)
[109]	1.50 ± 0.01 crossing over to 1.69 ± 0.04 with increasing N at fixed E (LD)
[158]	1.55 ± 0.04 (MC)
[115]	$2\nu = 1.5$

Table 3. Summary of all the reported values of the exponent for the pore-blockade time for field-driven translocation of a Rouse polymer in three dimensions, known to us at the time of writing this review. Abbreviations: LD (Langevin dynamics), MC (Monte Carlo).

References	α (3D, Rouse)
[110]	1.27
[159]	1.65 ± 0.08
[160]	1.42 ± 0.01 (MD, LD)
[128]	1.5 (FENE)
[148]	$\frac{(1+2\nu)}{1+\nu} \approx 1.37$
[161]	1.36 ± 0.01
[162]	1.36 ± 0.03 (MD)
[122]	$1.35 - 1.40$ (LD)

Although in our view the results for two dimensions can clearly be reconciled by energy conservation arguments [115], and the memory function approach at weak fields ($E < E^*$) and stem–flower/tension propagation/trumpet models at moderate to strong fields ($E > E^*$) in three dimensions, this is by no means the only interpretation. In two recent papers Ikonen *et al* [163, 164] reanalyzed some of their own older data as well as those of Lehtola *et al* [152]; using pore friction as a control variable in a Brownian dynamics tension propagation scheme, they collapsed all the data on a master curve to establish that all data points to the pore-blockade time scaled as $N^{1+\nu}$.[6]

One last, theoretically interesting remark: note that the value $\alpha = (1 + 2\nu)/(1 + \nu)$ for a Rouse polymer in three dimensions violates the expected lower limit $1 + \nu$ expected by Kantor and Kardar [140]. This is because the lower limit proposed by them is incorrect. This has been easily argued from energy conservation considerations [115, 150]. Consider a translocating Rouse polymer under a field E: N monomers take time τ_d to translocate through the pore. The total work done by the field in time τ_d is then given by EN. In time τ_d, each monomer travels a distance $\sim R_g \sim N^\nu$, the radius of gyration of the polymer, leading to an average monomer velocity $v_m \sim R_g/\tau_d$. The rate of loss of energy due to viscosity $\tilde{\eta}$ of the surrounding medium per monomer is given by $\tilde{\eta} v_m^2$. For a Rouse polymer, the frictional force on the entire polymer is a sum of frictional forces on individual monomers, leading to the total free energy loss due to the viscosity of the surrounding medium during the entire translocation event scaling as $\Delta F \sim N\tau_d \tilde{\eta} v_m^2 = N\tilde{\eta} R_g^2/\tau_d$. This loss of energy must be less than or equal to the total work done by the field EN, which yields us the inequality $\tau_d \geq \tilde{\eta} R_g^2/E = \tilde{\eta} N^{2\nu}/E$. In three dimensions $2\nu < (1 + 2\nu)/(1 + \nu)$, so the result that $\alpha = (1 + 2\nu)/(1 + \nu)$ for a Rouse polymer does not violate the lower limit (a similar argument leads to the result $\alpha = 3\nu/(1 + \nu)$ for a Zimm polymer which also does not violate the corresponding lower limit $3\nu - 1$).

In contrast to the above, field-driven translocation of Zimm polymers has been studied with much less intensity. The memory function approach predicts $\alpha = 3\nu/(1 + \nu) \approx 1.11$ which should only hold for weak fields [148]. Unlike Rouse polymers, field-driven translocation of Zimm polymers is accessible to experiments [72], reporting a pore-blockade time exponent 1.27 ± 0.03. The authors explained the exponent to be 2ν, based on a mechanistic picture wherein the polymer chain on the *cis* side moves as a macroscopic blob, as it gradually gets sucked into the pore. While such a mechanistic picture is unlikely to be correct, we note that simulation results confirming the numerical value of the exponent do exist ($\alpha = 1.28 \pm 0.01$) [162]. There is however another simulation study reporting $\alpha \approx 1.2$, claiming an agreement with $\alpha = 3\nu/(1 + \nu)$, the prediction from the memory function approach. The existence of E^* as distinguishing strong and weak field regimes, and the dependence of the pore-blockade time on the strength of the applied field have essentially not been addressed.

5.3. Translocation by pulling with optical tweezers

In this method of translocation a fluorescent bead is attached to one end of the polymer after the polymer is threaded through the pore. The bead is then captured by optical tweezers and as it is pulled away from the pore on the *trans* side, the rest of the polymer translocates through the pore. This experiment is motivated by the desire to determine the secondary structure of an RNA molecule (see [165] and the references cited therein).

Several groups have studied this problem for Rouse polymers, and $\tau_d \sim N^2$ has been unambiguously established [166, 167]—this is a rare case of agreement in this field. The memory function approach predicts this exponent [165]: on the *trans* side of the membrane the polymer achieves a stretched configuration, leading to a power-law memory in time that behaves as $t^{-1/2}$, while on the *cis* side the polymer's memory decays in time, for weak pulling force, as $t^{-(1+2\nu)/(1+\nu)}$. The first one, being the slower of the two, determines the pore-blockade time exponent. This picture is also confirmed by simulations of polymer translocation under a double force arrangement [168], and by pulling an adsorbed polymer away by an optical tweezers [169], a problem that can be mapped to translocation by a pulling force just like

[6] Further, the scatter in the dependence of pore-blockade time on E, reported in several simulation papers [147, 152, 155, 156, 164], is far too big to draw a definitive conclusion. Aside from the complications involving model parameters as noted above, it is not easy to let the field value span multiple decades such that a power-law dependence can be determined reliably, although there is a predominance of reporting $\tau_d \sim 1/E$.

the adsorption problem has been mapped on to field-driven translocation problem [150].

5.4. Epilogue to section 5

The reader should bear in mind that the purpose behind section 5 is not to provide an encyclopedic summary of all the translocation studies on pore-blockade times. Instead, the purpose is to present the generic problems that several research groups have concentrated on. There are many studies like polymer translocation through pores with complex geometries, such as [170, 171] as well as pioneering theoretical studies on protein translocation across nanopores using Langevin dynamics and molecular dynamics simulations [25, 172–177] that we have chosen to leave out. In this context we note that there are some interesting problems like zipping–unzipping dynamics of DNA strands that have been mapped on to translocation [178, 179]. To what extent these are related to translocation is, however, unclear.

6. Experimental aspects still in want of theoretical understanding

The number and variety of experimental investigations that target polymer dynamics aspects during translocation is constantly increasing. Many new techniques have recently been developed for uncovering mechanisms of transport through channels and nanopores, thus providing an increased amount of microscopic information on translocation processes. Some of these experimental studies have been addressed by theoretical work, but there is still a significant number of observations that need to be fully explained. In this section our goal is to highlight some of these polymer translocation phenomena that are still not well understood.

The success of current nanopore translocation methods is based on very precise measurements of current fluctuations of small ions during the experiments [2–6]. These fluctuations appear because fluxes of charged particles present in the system across the channel are different with and without the polymer in the pore. The majority of experiments have reported a drop in the current (a current blockade) when the polymer threads through the pore [3, 4]. It has been argued that these observations can be well understood since the polymer geometrically excludes some part of the channel from small cations and anions, reducing the overall flux of charged particles. However, a recent experiment on translocation of double-stranded DNA molecules through some solid-state nanopores reported a surprising increase in the channel current, observed at some sets of parameters [180], and these results have challenged existing views on nanopore sensing as a purely geometric exclusion phenomenon. It was shown that at low concentrations of the salt (specifically, KCl in experiments) the current during the translocation increases, while for large concentrations there are current blockades. Several phenomenological models of how the charged particle flux through nanopores can be enhanced have been proposed [180]. In particular, it was argued that the presence of a negatively charged DNA molecule attracts additional K^+ cations into the channel, and the overall current might increase. However, these approaches produced simplified and very qualitative descriptions that have led to many contradictions and questions. For example, if DNA attracts cations into the pore, why do these ions leave the channel? The strong attraction into the pore would lead to lowering the current, in contrast to observations in these experiments. Why does the attraction exist only for some sets of parameters, e.g., low-salt conditions? Why are these phenomena observed only for artificial solid-state nanopores, while dynamics in biological channels is more or less consistent with exclusion arguments? From these questions one can conclude that the microscopic origins of this unusual phenomenon are still far from being clear. This is a critical issue since all quantitative data on polymer translocation are associated with changes in currents of charged particles, which apparently are not understood.

Another important problem that needs to be resolved theoretically is connected with the role of polymer conformations during translocation. It is widely assumed that during the motion through the channel the polymer molecule moves as a linear chain in a ‘single-file’ fashion. However, experiments on solid-state nanopores suggest that in many cases the polymer translocates in the partially folded conformation [71, 72]. In this case, the polymer experiences spatially and temporally varying interactions with the pore, leading to complex dynamics. Similar problems are observed in experiments where the polymer adsorbs near the nanopore, modifying the current through the channel [181]. The translocation of folded polymers has been addressed theoretically, but only using the quasi-equilibrium phenomenological approach [182], while in this case one expects non-equilibrium phenomena to have a stronger influence on polymer dynamics. The important questions here are the following. (i) Are polymer folding conformations affecting the translocation dynamics? (ii) What is the role of polymer–pore interactions in this case? (iii) How is the channel geometry coupled to translocation of the folded polymers? It is important to develop a non-equilibrium approach that will address these important issues.

7. Perspective: the future of this field

In recent years, the field of polymer translocation has seen a fast growth with strong advances. It is now possible to observe single-molecule polymer dynamics during the motion through channels with unprecedented spatial and temporal resolution. These striking experimental studies stimulated many theoretical developments. However, although several ideas that underlie the non-equilibrium nature of polymer translocation have been introduced and tested in extensive theoretical and computer simulation studies, most experiments are still analyzed using over-simplified quasi-equilibrium theoretical methods. It is important to extend the non-equilibrium approaches to describe not only computer simulations but more importantly real polymer translocation phenomena (as in experiments). In

our opinion, this will be one of the most difficult challenges for the field.

Considering theoretical advances in translocation, one can see that several mechanisms to understand the deviations from equilibrium dynamics of threading polymers have been proposed and analyzed. Because of these developments many features of polymer transport through channels are now better understood. However, none of the existing methods can fully explain polymer dynamics in all parts of the parameters space. It suggests that there is a need to develop a unified comprehensive theoretical approach that will fully address all issues associated with the non-equilibrium nature of polymer translocation and that will be valid for all conditions. This will be another important goal for future theoretical studies on translocation. It is clear that future progress on understanding the mechanisms of polymer motion through channels and pores will strongly depend on combined theoretical and experimental efforts to analyze these complex phenomena.

Acknowledgments

We thank Takahiro Sakaue for detailed comments on the review, and the wider translocation community for many lively discussions. A B K acknowledges the support from the Welch Foundation (Grant C-1559).

References

[1] Lodish H *et al* 1995 *Molecular Cell Biology* 4th edn (New York: Scientific American Books)
[2] Muthukumar M 2011 *Polymer Translocation* (Boca Raton, FL: CRC Press)
[3] Zwolak M and Di Ventra M 2008 *Rev. Mod. Phys.* **80** 141
[4] Meller A 2003 *J. Phys.: Condens. Matter* **15** R581
[5] Aksimentiev A 2011 *Nanoscale* **2** 468
[6] Keyser U F 2011 *J. R. Soc. Interface* **8** 1369
[7] Dekker C 2007 *Nature Nanotechnol.* **2** 209
[8] Wanunu M *et al* 2008 *Biophys. J.* **95** 4716
[9] Maglia G *et al* 2008 *Proc. Natl Acad. Sci. USA* **105** 19720
[10] Liu H *et al* 2010 *Science* **327** 64
[11] Cockroft S L *et al* 2008 *J. Am. Chem. Soc.* **130** 818
[12] Lieberman K R *et al* 2010 *J. Am. Chem. Soc.* **132** 17961
[13] Newton M R *et al* 2006 *Langmuir* **22** 4429
[14] Mathe J *et al* 2005 *Proc. Natl Acad. Sci. USA* **102** 12377
[15] Matysiak S *et al* 2006 *Phys. Rev. Lett.* **96** 118103
[16] Muthukumar M 2003 *J. Chem. Phys.* **118** 5174
[17] Wong C T A and Muthukumar M 2008 *J. Chem. Phys.* **128** 154903
[18] Butler T Z *et al* 2006 *Biophys. J.* **90** 190
[19] Milchev A 2011 *J. Phys.: Condens. Matter* **23** 103101
[20] Deamer D W and Akeson M 2000 *Trends Biotechnol.* **18** 147
[21] Deamer D and Branton D 2002 *Acc. Chem. Res.* **35** 817
[22] Muthukumar M 2007 *Annu. Rev. Biophys. Biomol. Struct.* **36** 435
[23] Branton D *et al* 2008 *Nature Biotechnol.* **26** 1146
[24] Movileanu L 2008 *Soft Matter* **4** 925
[25] Makarov D E 2008 *Acc. Chem. Res.* **42** 281
[26] Movileanu L 2009 *Trends Biotechnol.* **27** 333
[27] Majd S *et al* 2010 *Curr. Opin. Biotechnol.* **21** 439
[28] Gu L Q *et al* 2012 *Expert Rev. Mol. Diagn.* **12** 573
[29] Rouse P E 1953 *J. Chem. Phys.* **21** 1272
[30] Zimm B H 1956 *J. Chem. Phys.* **24** 269
[31] Henrickson S E *et al* 2000 *Phys. Rev. Lett.* **85** 3057
[32] Meller A and Branton D 2002 *Electrophoresis* **23** 2583
[33] Brun L *et al* 2008 *Phys. Rev. Lett.* **100** 158302
[34] Fologea D *et al* 2005 *Nano Lett.* **5** 1734
[35] Kasianowicz J J *et al* 1996 *Proc. Natl Acad. Sci. USA* **93** 13770
[36] Akeson M *et al* 1999 *Biophys. J.* **77** 3227
[37] Meller A *et al* 2000 *Proc. Natl Acad. Sci. USA* **97** 1079
[38] Meller A, Nivon L and Branton D 2001 *Phys. Rev. Lett.* **86** 3435
[39] Howorka S *et al* 2001 *Proc. Natl Acad. Sci. USA* **98** 12996
[40] Sauer-Budge A F *et al* 2003 *Phys. Rev. Lett.* **90** 238101
[41] Mathe J *et al* 2004 *Biophys. J.* **87** 3205
[42] Wang H *et al* 2004 *Proc. Natl Acad. Sci. USA* **101** 13472
[43] Dudko O K *et al* 2007 *Biophys. J.* **92** 4188
[44] Butler T Z *et al* 2007 *Biophys. J.* **93** 3229
[45] Lin J, Kolomeisky A B and Meller A 2010 *Phys. Rev. Lett.* **104** 158101
[46] Vercoutere W *et al* 2001 *Nature Biotechnol.* **19** 248
[47] Hornblower B *et al* 2007 *Nature Methods* **4** 315
[48] Tabard-Cossa V *et al* 2009 *ACS Nano* **3** 3009
[49] Tropini C and Marziali A 2007 *Biophys. J.* **92** 1632
[50] Goodrich C P *et al* 2007 *J. Phys. Chem.* B **111** 3332
[51] Movileanu L *et al* 2005 *Biophys. J.* **89** 1030
[52] Sutherland T C *et al* 2004 *Nano Lett.* **4** 1273
[53] Sakaue T and Raphaël E 2006 *Macromolecules* **39** 2621
[54] Sakaue T 2007 *Macromolecules* **40** 5206
[55] Oukhaled G *et al* 2007 *Phys. Rev. Lett.* **98** 158101
[56] Wolfe A J *et al* 2007 *J. Am. Chem. Soc.* **129** 14034
[57] Bikwemu R *et al* 2010 *J. Phys.: Condens. Matter* **22** 454117
[58] Mohammad M M *et al* 2008 *J. Am. Chem. Soc.* **130** 4081
[59] Bezrukov S *et al* 1996 *Macromolecules* **29** 8517
[60] Movileanu L and Bayley H 2001 *Proc. Natl Acad. Sci. USA* **98** 10137
[61] Movileanu L *et al* 2003 *Biophys. J.* **85** 897
[62] Murphy R and Muthukumar M 2007 *J. Chem. Phys.* **126** 051101
[63] Oukhaled G *et al* 2008 *Europhys. Lett.* **82** 48003
[64] An N *et al* 2012 *Proc. Natl Acad. Sci. USA* **109** 11504
[65] Heng J B *et al* 2004 *Biophys. J.* **87** 2905
[66] Cheneke B R *et al* 2012 *Biochemistry* **51** 5348
[67] Mohammad M M *et al* 2012 *J. Am. Chem. Soc.* **134** 9521
[68] Manrao E A *et al* 2012 *Nature Biotechnol.* **4** 349
[69] Pavlenok M *et al* 2012 *PLoS One* **7** e38726
[70] Storm A J *et al* 2003 *Nature Mater.* **2** 537
[71] Storm A J *et al* 2005 *Phys. Rev.* E **71** 051903
[72] Storm A J *et al* 2005 *Nano Lett.* **5** 1193
[73] Heng J B *et al* 2005 *Nano Lett.* **5** 1883
[74] Keyser U F *et al* 2006 *Nature Phys.* **2** 473
[75] Heng J B *et al* 2006 *Biophys. J.* **90** 1098
[76] Trepagnier E H *et al* 2007 *Nano Lett.* **7** 2824
[77] McNally B *et al* 2008 *Nano Lett.* **8** 3418
[78] Smeets R M M *et al* 2008 *Proc. Natl Acad. Sci. USA* **105** 417
[79] Lu B *et al* 2011 *Biophys. J.* **101** 70
[80] Li J *et al* 2001 *Nature* **412** 166
[81] Li J *et al* 2003 *Nature Mater.* **2** 611
[82] Stein D, Li J and Golovchenko J A 2002 *Phys. Rev. Lett.* **89** 276106
[83] Niedzwiecki D J, Grazul J and Movileanu L 2010 *J. Am. Chem. Soc.* **132** 10816
[84] Niedzwiecki D J *et al* 2013 *ACS Nano* **7** 3341
[85] Wanunu M *et al* 2010 *Nature Nanotechnol.* **5** 160
[86] Merchant C A *et al* 2010 *Nano Lett.* **10** 2195
[87] Lee C Y *et al* 2010 *Science* **329** 1320
[88] Russo C J and Golovchenko J A 2012 *Proc. Natl Acad. Sci. USA* **109** 5953
[89] Garaj S *et al* 2010 *Nature* **467** 190
[90] Schneider G F *et al* 2010 *Nano Lett.* **10** 3163
[91] Venkatesan B M *et al* 2012 *ACS Nano* **6** 441
[92] Cichelli J and Zharov I 2006 *J. Am. Chem. Soc.* **128** 8130
[93] Mirsaidov U *et al* 2009 *Biophys. J.* **96** L32

[94] Howorka S and Bayley H 2002 *Biophys. J.* **83** 3202
[95] Robertson J W F *et al* 2007 *Proc. Natl Acad. Sci. USA* **104** 8207
[96] Reiner J E *et al* 2010 *Proc. Natl Acad. Sci. USA* **107** 12080
[97] Baaken G *et al* 2011 *ACS Nano* **5** 8080
[98] Diehl H W and Shpot M 1998 *Nucl. Phys.* B **528** 595
[99] Chen P *et al* 2004 *Nano Lett.* **4** 2293
[100] Hatlo M M, Panja D and van Roij R 2011 *Phys. Rev. Lett.* **107** 068101
[101] Wong C T A and Muthukumar M 2007 *J. Chem. Phys.* **126** 164903
[102] Wolterink J K, Barkema G T and Panja D 2006 *Phys. Rev. Lett.* **96** 208301
[103] Sung W and Park P J 1996 *Phys. Rev. Lett.* **77** 783
[104] Muthukumar M 1999 *J. Chem. Phys.* **111** 10371
[105] Slonkina E and Kolomeisky A B 2003 *J. Chem. Phys.* **118** 7112
[106] Chuang J, Kantor Y and Kardar M 2002 *Phys. Rev.* E **65** 011802
[107] Carmesin I and Kremer K 1988 *Macromolecules* **21** 2819
[108] Luo K *et al* 2006 *J. Chem. Phys.* **124** 034714
[109] Huopaniemi I *et al* 2006 *J. Chem. Phys.* **125** 124901
[110] Wei D *et al* 2007 *J. Chem. Phys.* **126** 204901
[111] Chatelain C, Kantor Y and Kardar M 2008 *Phys. Rev.* E **78** 021129
[112] Luo K *et al* 2008 *Phys. Rev.* E **78** 050901
[113] Panja D, Barkema G T and Ball R C 2007 *J. Phys.: Condens. Matter* **19** 432202
[114] Panja D, Barkema G T and Ball R C 2006 arxiv:cond-mat/0610671
[115] Panja D, Barkema G T and Ball R C 2008 *J. Phys.: Condens. Matter* **20** 075101
[116] Dubbeldam J L A *et al* 2007 *Phys. Rev.* E **76** 010801
[117] Gauthier M G and Slater G W 2008 *J. Chem. Phys.* **128** 205103
[118] Guillouzic S and Slater G W 2006 *Phys. Lett.* A **359** 261
[119] Gauthier M G and Slater G W 2008 *Eur. Phys. J.* E **25** 17
[120] Kapahnke F *et al* 2010 *J. Chem. Phys.* **132** 164904
[121] de Haan H and Slater G W 2012 *J. Chem. Phys.* **136** 154903
[122] Edmonds C M *et al* 2012 *J. Chem. Phys.* **136** 065105
[123] Bird B *et al* 1977 *Dynamics of Polymeric Liquids* (*Kinetic Theory*) vol 2 (New York: Wiley)
[124] Jiang W H *et al* 2007 *J. Chem. Phys.* **126** 044901
[125] Panja D 2009 *Phys. Rev.* E **79** 011803
[126] Metzler R and Klafter J 2003 *Biophys. J.* **85** 2776
[127] Lua R C and Grosberg A Y 2005 *Phys. Rev.* E **72** 061918
[128] Dubbeldam J L A *et al* 2007 *Europhys. Lett.* **79** 18002
[129] Panja D 2010 *J. Stat. Mech.* L02001
[130] Panja D 2010 *J. Stat. Mech.* P06011
[131] Panja D 2011 *J. Phys.: Condens. Matter* **23** 105103
[132] Dubbeldam J L A *et al* 2011 *Phys. Rev.* E **83** 011802
[133] Panja D and Barkema G T 2010 *J. Chem. Phys.* **132** 014902
[134] de Haan H and Slater G W 2012 *J. Chem. Phys.* **136** 204902
[135] Slater G W 2012 personal communication
[136] Lubensky D K and Nelson D R 1999 *Biophys. J.* **77** 1824
[137] Park P J and Sung W 1998 *Phys. Rev.* E **57** 730
[138] Muthukumar M 2001 *Phys. Rev. Lett.* **86** 3188
[139] Park P J and Sung W 1998 *J. Chem. Phys.* **108** 3013
[140] Kantor Y and Kardar M 2004 *Phys. Rev.* E **69** 021806
[141] Sakaue T 2007 *Phys. Rev.* E **76** 021803
[142] Sakaue T 2010 *Phys. Rev.* E **81** 041808
[143] Saito T and Sakaue T 2011 *Eur. Phys. J.* E **34** 135
[144] Saito T and Sakaue T 2012 *Eur. Phys. J.* E **35** 125
[145] Sakaue T, Saito T and Wada H 2012 *Phys. Rev.* E **86** 011804
[146] Rowghanian P and Grosberg A Y 2011 *J. Phys. Chem.* B **115** 14127
[147] Dubbeldam J L A *et al* 2012 *Phys. Rev.* E **85** 041801
[148] Vocks H *et al* 2008 *J. Phys.: Condens. Matter* **20** 095224
[149] Sakaue T 2013 *Phys. Rev.* E **87** 040601
[150] Panja D, Barkema G T and Kolomeisky A B 2009 *J. Phys.: Condens. Matter* **21** 242101
[151] Brochard-Wyart F 1995 *Europhys. Lett.* **30** 387
[152] Lehtola V V, Linna R P and Kaski K 2008 *Phys. Rev.* E **78** 061803
[153] Lehtola V V, Linna R P and Kaski K 2009 *Europhys. Lett.* **85** 58006
[154] Lehtola V V, Linna R P and Kaski K 2010 *Phys. Rev.* E **81** 031803
[155] Luo K *et al* 2009 *Europhys. Lett.* **88** 68006
[156] Metzler R and Luo K 2010 *Eur. Phys. J. Spec. Top.* **189** 119
[157] Luo K *et al* 2006 *J. Chem. Phys.* **124** 114704
[158] Cacciuto A and Luijten E 2006 *Phys. Rev. Lett.* **96** 238104
[159] Milchev A, Binder K and Bhattacharya A 2004 *J. Chem. Phys.* **121** 6042
[160] Luo K *et al* 2008 *Phys. Rev.* E **78** 050901
[161] Bhattacharya A *et al* 2009 *Eur. Phys. J.* E **29** 423
[162] Fyta M *et al* 2008 *Phys. Rev.* E **78** 036704
[163] Ikonen T *et al* 2012 *Phys. Rev.* E **85** 051803
[164] Ikonen T *et al* 2012 *J. Chem. Phys.* **137** 085101
[165] Vocks H, Panja D and Barkema G T 2009 *J. Phys.: Condens. Matter* **21** 375105
[166] Huopaniemi I *et al* 2007 *Phys. Rev.* E **75** 061912
[167] Panja D and Barkema G T 2008 *Biophys. J.* **94** 1630
[168] Ollila S T T *et al* 2009 *Eur. Phys. J.* E **28** 385
[169] Paturej J *et al* 2012 *Macromolecules* **45** 4371
[170] Mohan A, Kolomeisky A B and Pasquali M 2010 *J. Chem. Phys.* **133** 024902
[171] Wong C T and Muthukumar M 2008 *J. Chem. Phys.* **128** 154903
[172] Tian P and Andricioaei I 2005 *J. Mol. Biol.* **350** 1017
[173] Huang L, Kirmizialtin S and Makarov D E 2005 *J. Chem. Phys.* **123** 124903
[174] Huang L and Makarov D E 2008 *J. Chem. Phys.* **128** 114903
[175] Huang L and Makarov D E 2008 *J. Chem. Phys.* **129** 121107
[176] Kirmizialtin S, Ganesan V and Makarov D E 2004 *J. Chem. Phys.* **121** 10268
[177] Kirmizialtin S, Huang L and Makarov D E 2006 *Phys. Status Solidi* b **243** 2038
[178] Ferrantini A, Baiesi M and Carlon E 2010 *J. Stat. Mech.* P03017
[179] Ferrantini A and Carlon E 2011 *J. Stat. Mech.* P02020
[180] Smeets R M M *et al* 2006 *Nano Lett.* **6** 89
[181] Vlassarev D M and Golovchenko J A 2012 *Biophys. J.* **103** 352
[182] Kotsev S and Kolomeisky A B 2007 *J. Chem. Phys.* **127** 185103